Probability of Overlap for Footprints of Satellites Flying in Formation

Mark A. Vincent
Jet Propulsion Laboratory
California Institute of Technology

Summary

The general problem of determining footprint overlap for instruments on different platforms was analyzed by determining the formation flying and pointing requirements needed to satisfy the science requirements of the Cloudat and PICASSO-CENA missions. A control value of +/-1 km was found to satisfy the requirement of keeping the footprints within 2 km of each other. If the pointing errors are considered as pure random variables this control results in a 71% probability of footprint overlap. However, if the pointing errors a considered to be fixed biases, the difference between the crosstrack bias values must be less than the sum of the footprint half-widths in order to reach the goal of the footprints overlapping 50% of the time. Satisfying this limit has an 81% probability of occurrence. Combining both a bias and various noise levels indicated that the 50% overlap criterion is independent of the noise. For lower bias values the noise decreases the likelihood of overlap but the noise has the opposite effect for higher bias values. The effect of having a tighter control band on the overlap probability was also studied.

Introduction

The future trend in Earth System science is to have multiple satellites rather than multiple instruments on large platforms. Even the measurements from the large EOS platforms will be combined with observations from separate satellites. Since there is usually an upper limit on the time difference allowed between the observations of the same region, some sort of formation flying is required to meet both the spatial and temporal requirements. Another application, perhaps even more stringent, is the calibration of an instrument sent up on a new platform to replace the measurements of an existing instrument.

This analysis involves the relationship between the footprints of the Cloudsat (CS) Cloud Profiling Radar (CPR) and the PICASSO-CENA (PC) Lidar. It addresses the following Science Requirement and Science Goal:

- For all points along the PC groundtrack, the edge of the nearest CS CPR footprint shall fall within 2 km of the edge of the nearest PC Lidar footprint on the same rev with a two-sided 3σ probability (≡ 99.73%)
- There is a goal to have the footprints overlapping at least 50% of the time

Method of Investigation

Referring to Figure 1, there are five variables and parameters to consider when discussing the separation of the footprint edges. If d is the distance between the edges:

$$d = | x + z_R(\mu_R, \sigma_R) - z_L(\mu_L, \sigma_L) | - 700 - 35.25$$

where x is crosstrack position of the CS groundtrack with respect to that of PC. The maximum of x is X and the 700 and 35.25 represent the half-widths of the CS and PC swaths respectively in meters. The random variable $z_L(\mu_L, \sigma_L)$ represents the pointing offset of the lidar aboard PC. It is assumed to be normally distributed with a mean μ_L and a standard deviation of σ_L. Note that although a non-normal distribution might affect the results it would be somewhat easily factored into this analysis. The pointing of the CPR is represented by a similar variable $z_R(\mu_R, \sigma_R)$.

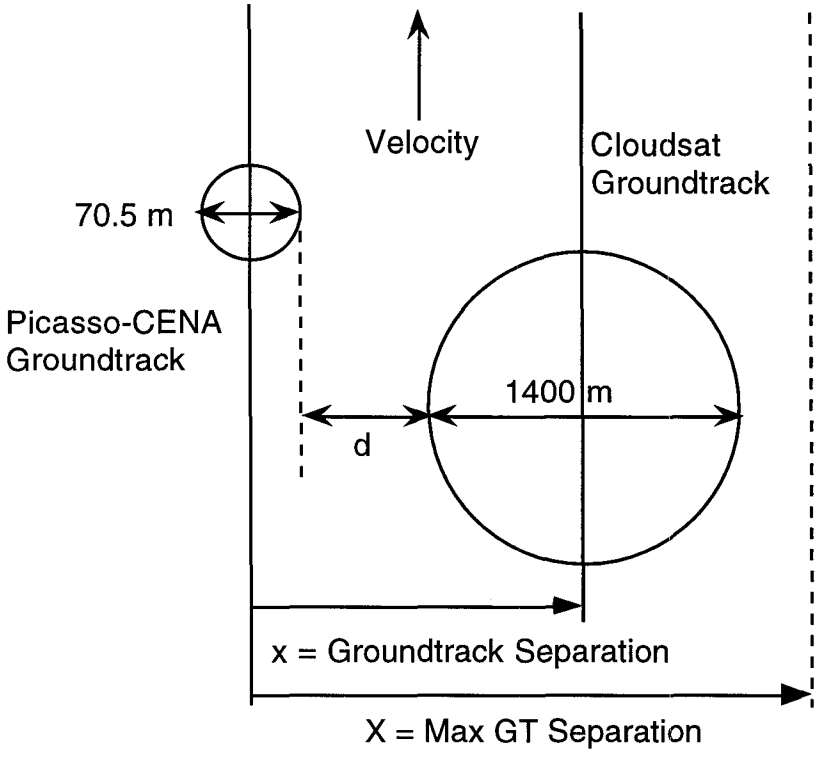

Footprint Geometry with No Pointing Errors
Figure 1

The analysis was divided into five parts. The first part addressed the 2 km between edges requirement. It is a separate, but necessary step before addressing the overlap probability issue. Using the resultant formation flying requirement, the overlap was determined by first assuming the pointing errors were white noise with the means μ_L and μ_R assumed to be zero. Next a fixed bias in the relative pointing was assumed with the same statistics. Then a combination of a bias and a variety of noise values was analyzed. Finally a tighter formation scenario, reflecting the practical case of including atmospheric drag uncertainty, was used for the combination bias/noise case.

A CPR crosstrack pointing error budget is 0.064° at the 3σ level was used, corresponding to 795 m, or a one-sigma value of σ_R = 265 m. Similarly, the lidar has a 3σ value of 1500 m and thus σ_L = 500 m. The first step is to convolute the two normal distributions by root-sum-squaring the standard deviations, giving a combined σ = 565.9 m and maintaining a zero mean. This simplifies the previous equation for d to be:

$$d = | x + z(0,565.9) | - 735.25$$

Substituting the 2 km boundary requirement for d, and X for x produces:

$$2000 > | X + z(0,565.9) | - 735.25$$

Since this requirement is at the 3σ level, the value 1698 m can be substituted for the z variable leaving X < 1038 m. For convenience and conservatism this number was rounded down to 1 km. Thus the derived requirement is:

The Cloudsat groundtrack must be maintained within +/- 1 km of the PICASSO-CENA groundtrack in the cross-track direction to insure that the edges of their footprints remain within 2 km of each other.

Doing the probability distribution function (pdf) convolution also allows the interesting pictorial explanation of both the calculation of X and the probability of overlap discussed below. As the value of x is increased, the two outside vertical lines on the right figure of Figure 2 shift to the left. When the red-hatched area is equal to the compliment of a (one-sided) 3σ probability, x is equal to X (one-sided because x = -X must also be accounted for). With the left vertical fixed, as the value of |x| varies during the maneuver cycle (as discussed below) the probability of overlap (green-hatched area) varies accordingly. Note that figures are valid for the entire +/- X range for x, with the caveat that when |x| < 735.35 (so that the CS pdf is to the left of the PC pdf), the green-hatched area on the left figure represents the probability of not overlapping.

To consider the overall probability of the footprint overlap, several assumptions as to the navigation control scheme and the behavior of the two groundtracks have to made. Subsequent analysis by D. Chart where he actually integrated the orbits and calculated the groundtracks, has verified these assumptions.

Atmospheric drag will affect both PC and CS by decreasing their semi-major axes (sma's). Due to different ballistic coefficients, there will be a differential effect in the SMA decrease, PC falling faster than CS. The idealized case used in this analysis assumed a maneuver is performed to make the CS sma about 100 m below that of PC when the CS groundtrack (gt) is on the western 1 km boundary with respect to the PC gt. Being in a lower orbit implies that the CS gt will move eastward with respect to the PC gt. Using the current estimates of the difference in ballistic coefficients a half a week later, the CS sma will be the same as that of PC and the CS gt will be on the eastern boundary.

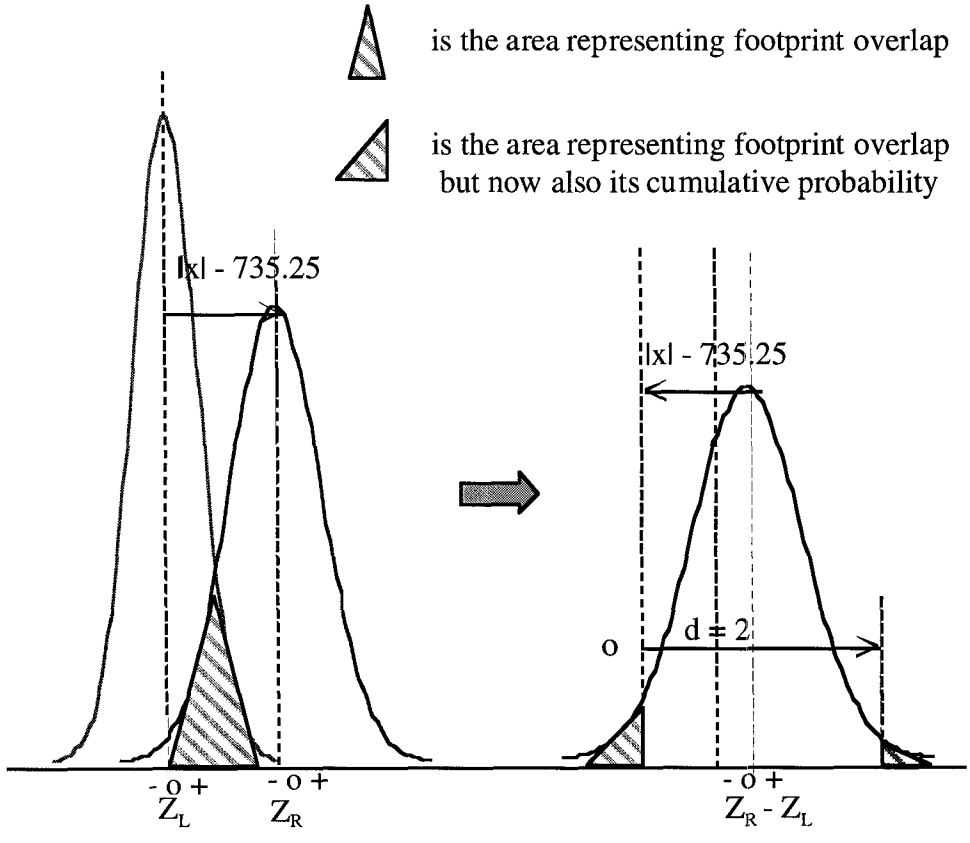

represents probability of d be greater than 2 km,
thus when it equals 0.135%, x = X, its allowable maximum

Convolution of the Cloudsat and PICASSO-CENA Probability Distribution Functions
Figure 2

Atmospheric drag will affect both PC and CS by decreasing their semi-major axes (sma's). Due to different ballistic coefficients, there will be a differential effect in the SMA decrease, PC falling faster than CS. The idealized case used in this analysis assumed a maneuver is performed to make the CS sma about 100 m below that of PC when the CS groundtrack (gt) is on the western 1 km boundary with respect to the PC gt. Being in a lower orbit implies that the CS gt will move eastward with respect to the PC gt. Using the current estimates of the difference in ballistic coefficients (note all these details will be given in a separate memo) a half a week later, the CS sma will be the same as that of PC and the CS gt will be on the eastern boundary.

Note that the atmospheric density was assumed constant at an extreme value corresponding to a geometric storm. More reasonable density values would result in less frequent maneuvers and smaller excursions in sma but the same excursions in gt differences so the following results would still hold. The constant density implies a linear change in sma and a quadratic change along-track the orbit corresponding to also a quadratic change in gt cross-track. After the half-week epoch CS's sma would be above PC's and the gt would drift westward. At the end of the week the initial conditions would be reoccur necessitating another identical maneuver.

Since the two satellite inclinations are identical, the separation discussed above refers to the orbital maximum separation which occurs at the equator crossings. If CS is east of PC , it will be to the right of PC at the ascending node, cross paths at the maximum latitude and be on the left side of PC at the descending node. Rather than integrating orbits and comparing gt's the following model was used to represent the cross-track position of the CS gt with respect to the PC gt.

$$x = (-787350 * (t-5040)^2 + 1000) * \sin(2\pi t / 98.8777)$$

where x is the cross-track separation distance in meters (note its maximum value is the X derived above). The time in minutes is designated by t and the orbital period is fixed at the 98.8777 value. The latter designation is an approximation in itself since even with perfect two-body plus constant drag model assumed so far, the period will vary slightly as the CS sma changes.

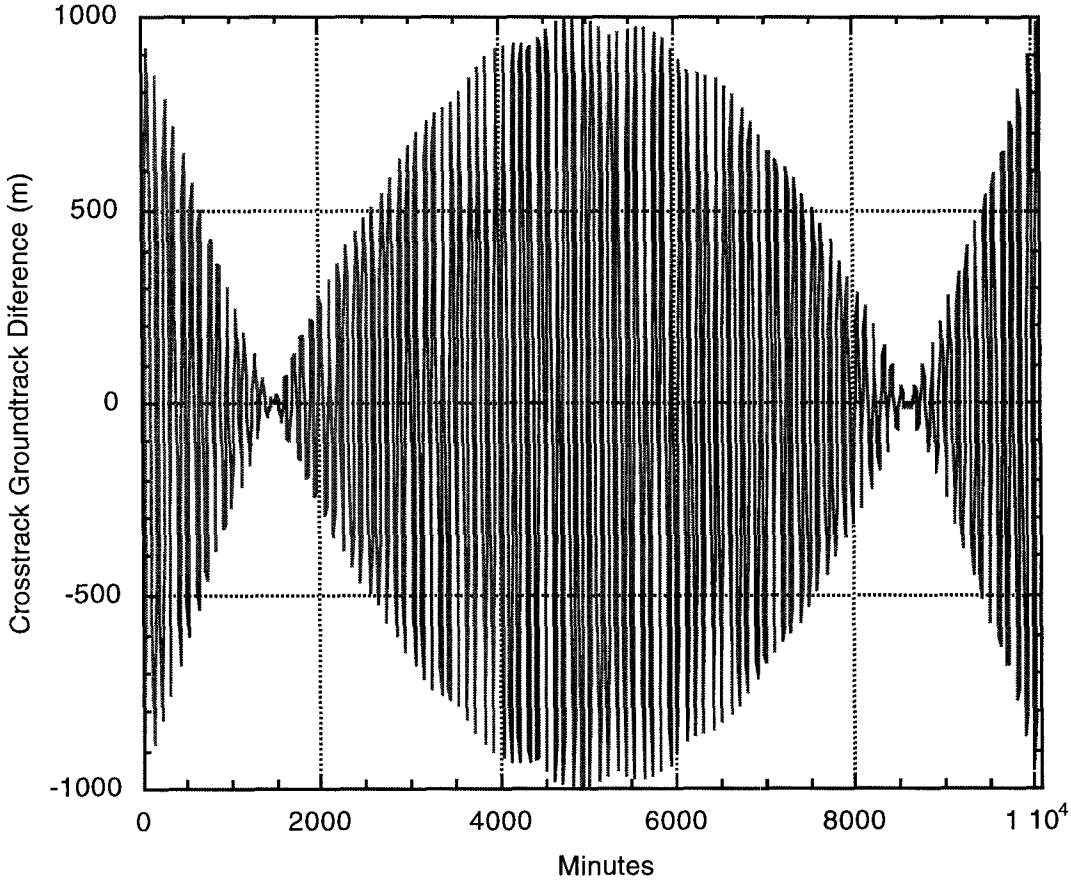

Simulated Crosstrack Differences
Figure 3

However, again this simulation should suffice to get the desired results. The results of running this model for a full week starting at the maneuver are shown in Figure 3. The combination of the quadratic long-term and sinusoidal once-per-rev signals is evident in the figure.

Results

Again using the above formalism for the separation distance d, it can be set to zero to represent the onset of overlap. Then for any given value of x, the probability of overlap is represented by:

$$z(0,565.9) < 735.25 - |x|$$

where the absolute value must be used because again we are concerned about the separation distance. The following table gives some examples for clarity:

Table 1
Probability of Overlap for some chosen x values (Noise Only)

x (m)	z_{max} (m)	Std z_{max} (σ)	Probability
0	735.25	1.299	90 %
735.25	0	0	50 %
1000	-264.75	-0.4678	32 %

These values can be verified by again looking at Figure 2 and substituting the values of x into the right-hand figure. However, a better illustration of how the probability varies throughout the cycle is shown in Figure 4. Here the probability values in blue are overlaid on the x values from Figure 3. The method creating the blue curve is described in the next paragraph.

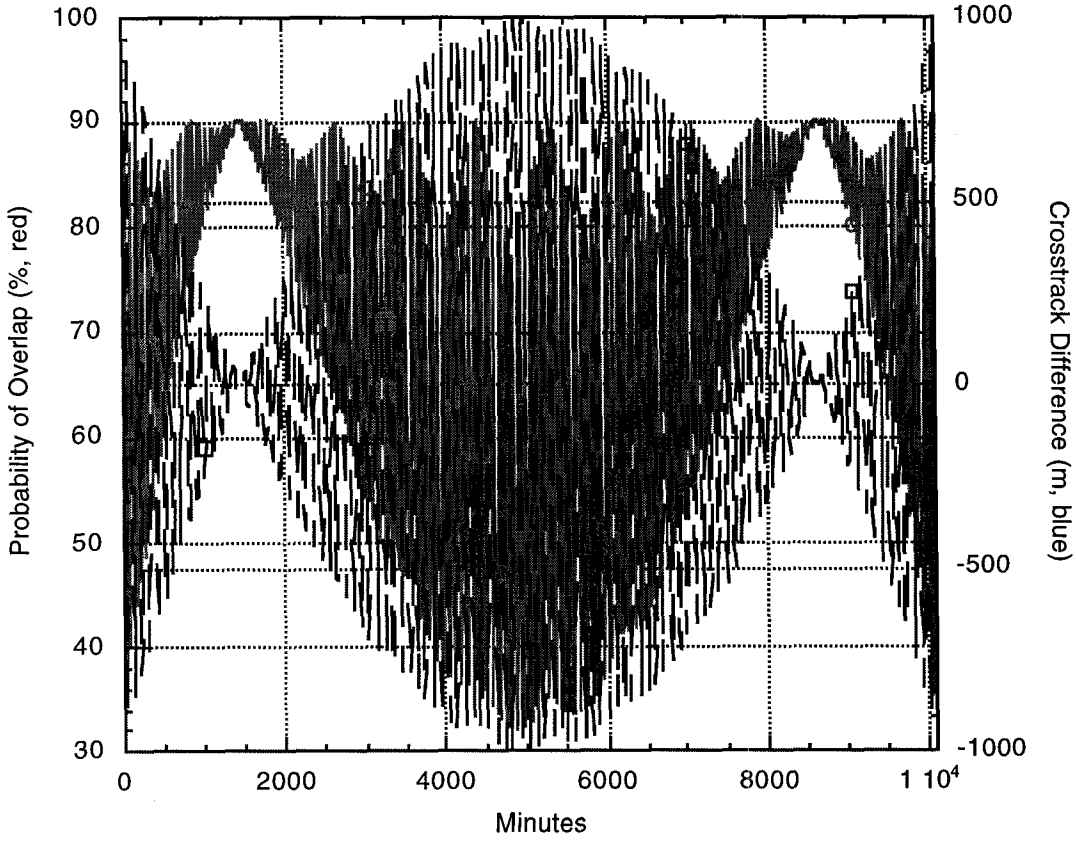

Probability of Overlap throughout a Cycle
Figure 4

The next step is to see what the effective probability is over one complete maneuver cycle. Although an analytical integral may have been possible, it was decided to do this numerically. Using the same 1008 10-minute points for x that were used to create Figure 3, a spreadsheet was used to calculate all the corresponding z_{max}'s and probabilities (and thus the blue curve in Figure 4). Summing and dividing by 1008 to get the average gave a value of 71% for the probability of overlap. If the pointing offsets were actual rapidly changing random variables, then not only would the probability of overlap for an arbitrary time be 71% but as the mission progresses the accumulative time of overlap would also tend toward this number.

In actuality, the pointing offsets could be slowly varying or have a fixed component corresponding to the mean offsets (μ's) mentioned previously. First an analysis looked at the case of fixed biases, followed by the cases of fixed plus random noise. A variable B was introduced to represent the bias offset difference between the lidar and radar. It is assumed to have the same statistics as z (since $z_L - z_R$ has the same statistics as $z_L + z_R$) but is considered fixed throughout the maneuver cycle. For the bias-only case, consider

$$d = | x + B | - 735.25$$

where again d is the distance between the edges of the footprints. Different values of B can be chosen and then using a similar process to that used above, the 1008 values of x can be substituted so statistics for d can be produced for a full cycle. Negative values for d correspond to overlap. Interesting results were obtained and shown in Figure 5. (Note the curve would have been smoother if more bias values had been looked at.) First consider no bias, B = 0, where the percentage of overlap is 84%. This is an important statistic since it represents the limit of no bias and no random noise. Next consider the goal of having 50% overlap. From the figure this occurs with the magnitude of the bias being at its 80.55 percentile but more pertinent this occurs when B = 735.25 m. This makes sense heuristically since overlap then occurs when x is the same sign as B and x behaves symmetrically. Further it suggests a goal to the instrument designers:

If the crosstrack component of the offset bias of each instrument can be limited to less than the half-cone angle of their footprint, 50% overlap of the footprints can be ensured (ignoring the random component).

For the CPR, 700 m is reasonable compared to the total (3σ) pointing error budget of 795 m. However, 35.25 represents a tight bias control compared to the current value of 1500 m for the total pointing error for the lidar. (Note that in PC presentations subsequent to this analysis, they have indicated much better overall pointing control error budgets).

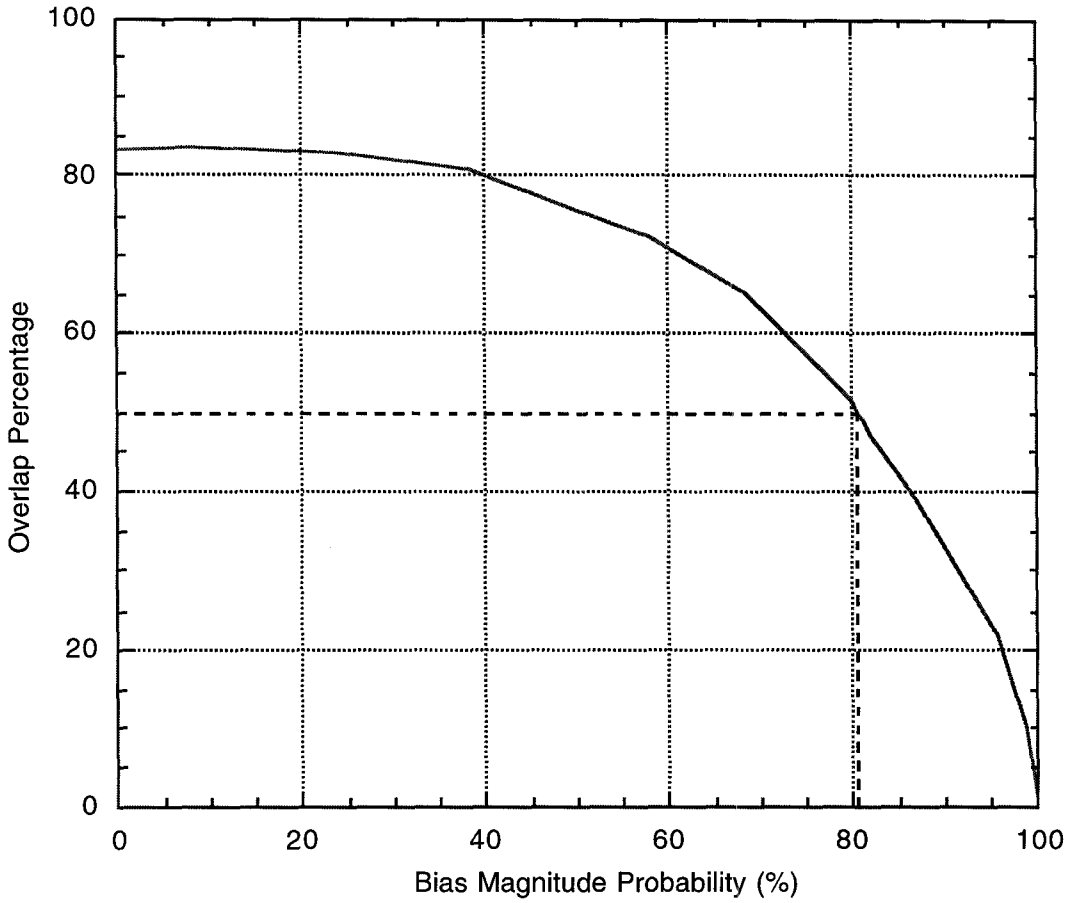

Footprint Overlap as a Function of Bias Magnitude
Figure 5

The next step was to combine the bias and noise models. For each of the same bias values, noise values were included. Specifically 50% (blue curve) and 100% (green curve) of the original standard deviation were picked and shown in Figure 6. The method used to calculate the probability of overlap was similar to that for the noise-only case, that is, find the average probability of overlap over the 1008 x values. In this case

$$d = | x + z(B,565.9) | - 735.25$$

However, it is worth noting that the methods used for the noise-only and bias-only are actually the same. When d is negative during the bias method it can be considered to have a 100% probability of overlap and likewise a positive value corresponds to 0%. Therefore the average probability is the same as the proportion of negative values times 100. If n is the number of negative values, this can be represented mathematically as:

$$[(n)\ 100\% + (1008\text{-}n)\ 0\%]/1008 = (n/1008)\ 100\%.$$

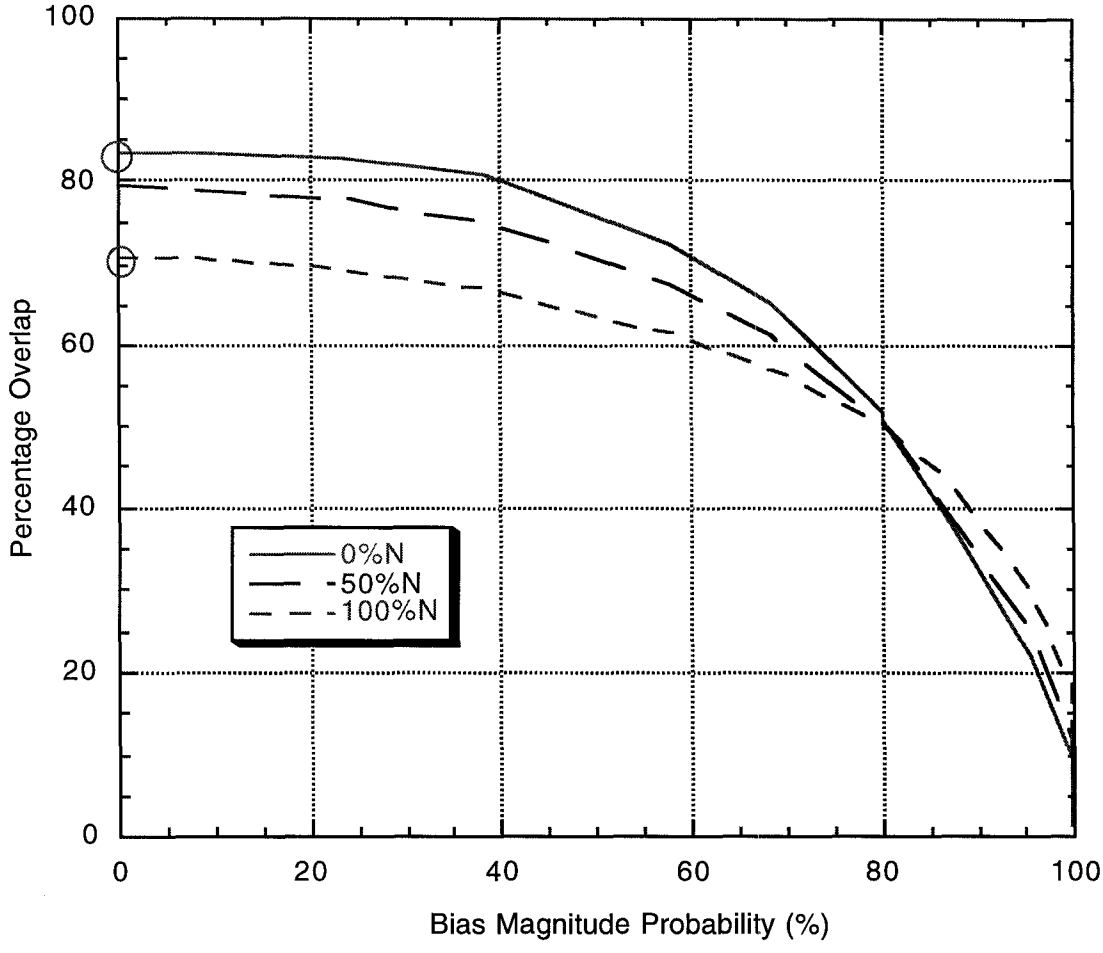

Probability of Overlap with both Bias and Noise
Figure 6

The results shown in Figure 6 were again interesting. The red circle is the probability of overlap with no bias or noise. The green circle represents the no-bias and 100% noise value determined earlier. The 50% percentage of overlap still corresponds to a bias magnitude that has a 81% probability of occurrence and is independent of the noise. Heuristically, it is best to think of the analogy to a simple normal zero-mean distribution curve. The probability of the random variable being negative or positive is 50% and is independent of the standard deviation of the variable. Away from this special value, the noise decreases the percentage of overlap for lower bias magnitude (probability) but the noise has the opposite effect for higher values. Again, there is an analogy, this time with two overlapping normal curves. When the means are close, increasing either sigma decreases the overlap but when the means are far apart, increasing either sigma increases the probability of overlap.

The final step was to account for the fact that in actuality the crosstrack variation of the nadir points will not be at it's maximum value of one kilometer. The method of designing maneuvers to not exceed these boundaries is the subject of another analysis. The general idea is to aim for a considerably smaller offset target so that uncertainties in solar activity and the resultant changes in atmospheric density do not cause the constraints to be violated. In order to best represent the range of possibilities it was decided to create the curves where there was no crosstrack variation. That is, the overlap is entirely dependent upon the pointing errors. Overlaying these results with those obtained previous obtained the useful regions depicted in Figure 7.

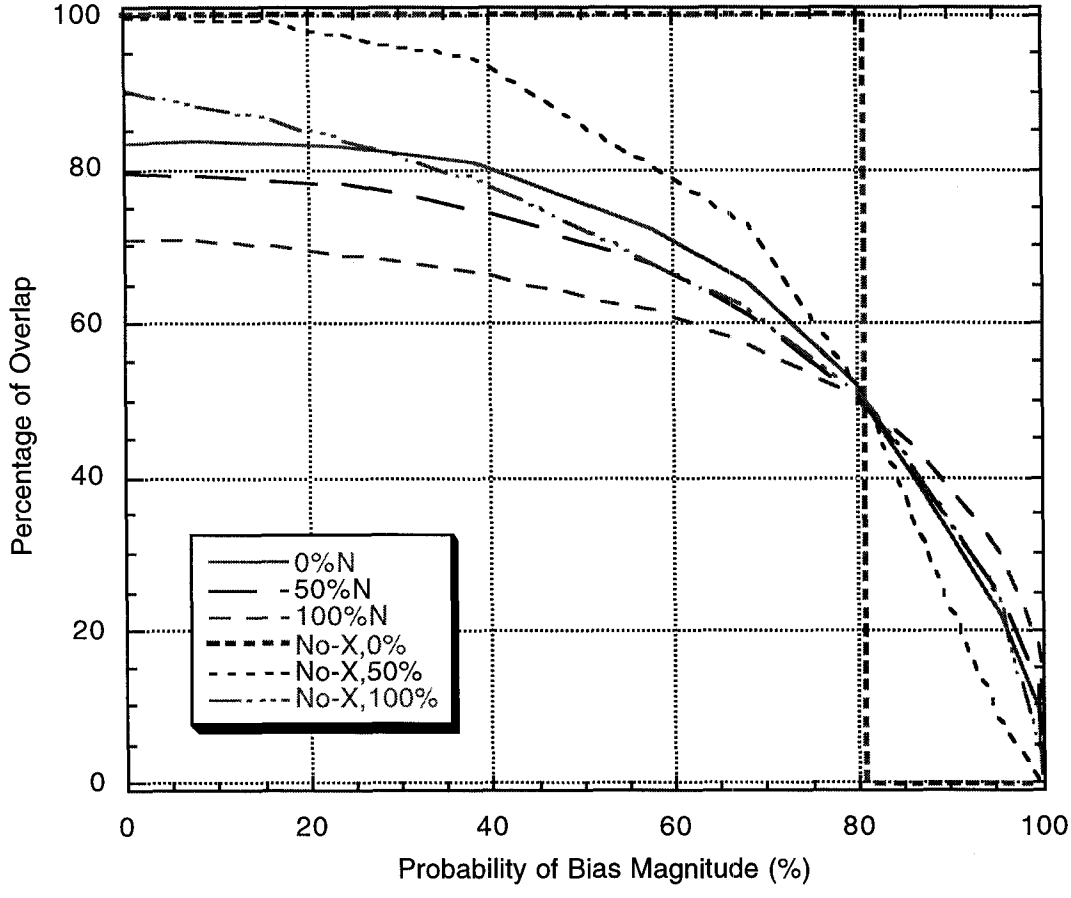

Probability of Overlap with Bias, Noise and Crosstrack Excursions
Figure 7

The area between the green lines represents the results for a Noise value of 100% with a variation from 1 km crosstrack excursion on one edge of the region to zero excursion on the other. Likewise for the blue lines (50% Noise) and red lines (0% Noise). The edge of the latter case representing no noise

and no excursion clearly indicates the concept of the bias being less than the half-width sum (always overlapped) versus the bias being greater than this value (never overlapped).

Conclusions

The straightforward result that a control requirement of +/- 1 km ensures a 3-sigma satisfaction of the "2-km between footprints edges" requirement was used for the subsequent maneuver design strategy formulation. The scientific community was pleased with an 81% probability of obtaining 50% overlap assuming that the bias difference in the instruments can be kept less than the sum of the half-widths of the footprints. The pointing error budgets will be further evaluated as the spacecraft bus and instrument designs for both missions mature. One aspect not mentioned yet is the assumptions of normality in the pointing error components. Even though this assumption is still believed to be valid, it is worth noting that an analysis similar to that presented above could be repeated with non-normal distributions.